Development of Inertial Measurement Sensor Using Magnetic Levitation

Young D. Kim*

Micro-Technology, Seoul, Korea

Kyeum R. Cho and **Dae W. Lee***

Department of Aerospace Engineering,
Pusan National University, Research Institute of Mechanical
Technology, Pusan, Korea 609-735

Abstract

An INS(Inertial Navigation System) is composed of a navigation computer and an IMU(Inertial Measurement Unit), and can be applied to estimate a vehicle's state. But the inertial sensors assembled in the IMU are too complicated and expensive to use for the general application purpose. In this study, a new concept of inertial sensor system using magnetic levitation is proposed. The proposed system is expected to replace one single-axis rate or position gyroscope, and one single-axis accelerometer concurrently with a relatively simple structure. A simulation of the proposed system is given to describe the capability of this new concept.

Introduction

A magnetic levitation system(Choi and Baek, 2002; Park et al., 1995) can be applied to precision position control equipment, high-speed magnetic bearings, and mechanical heart actuators to prevent a blood corpuscle from damage. The advantage of such a system is that an instrument may be supported with a minimum friction force and in the absence of a physical contact surface. Friction factors for this case are associated with magnetic eddy current damping, the unbalance problem of processing, and air drag, etc. But in the case where relevant motion is small, it is possible to make ideal frictionless situations due to several technical considerations. Recently, by using this property, there was research (Park et al., 1998) related to sensors that measure the motion of transportation. The work done is of mainly academic use because there is no consideration of rotational motion and it is fundamentally necessary to compensate for the three dimensional motion. In this research, by using one magnetic system we propose to measure angular motion and linear acceleration about a single axis. A cone-shaped cylinder can be levitated around an equilibrium point by magnetic force and a couple of four magnetic-pairs at each end. Therefore, we can control five degrees of freedom, which is the motion of the X, Y, Z translational directions, and the Y, Z rotational directions motion with a minimum of eight

magnets (Jung, 1998). In this system, we assume disturbances are the linear acceleration $\underline{a}$ and

the angular acceleration $\underline{\alpha}$ from the outside. Neglecting disturbances, the levitated magnetic body can move from the equilibrium point if the disturbances disappear, it returns to the equilibrium point.

* Graduate Student
** Professor
*** Assistant Professor
   E-mail : baenggi@pusan.ac.kr,   Tel: 051-510-2329,   Fax: 051-513-3760

At this moment the displacement can be divided into the translational displacement by the linear acceleration, and the rotational displacement by the angular acceleration. Hence, if we control to increase the linear acceleration with the infinitesimal displacement of the magnet's X direction and eliminate the acceleration disturbance in the remaining directions, we can get the linear acceleration in the X-direction. Also, under this condition, if we measure the relevant angle between the outer frame of the system and the levitated magnet, we can measure the angular motion about the X direction. That is, the gyroscope maintains the inertial attitude due to the gyroscopic stiffness of an object rotating with high speed, while this system measures attitude due to the inertia of the levitated magnet with the frictionless support.

The controller is designed to separate the state equations of this system into the translational motion of the X-axis and the remaining motion modes. For the X-axis direction translational motion mode, this system is designed to have a desired damping ratio and natural frequency with feedback using position stiffness and current stiffness coefficients. Then for the axis direction acceleration component, the displacement indicates the acceleration. Also for the Y, Z-axis direction translational and rotational motion modes, the magnetic levitation system can reach a zero steady state error for disturbance by using the LQG/LTR technique with free integral action. We considered the low sensitivity of the sensor and the robustness as well as the disturbance rejection.

System Modeling

2.1 System Configuration

Fig. 1 shows the composition of the system. The ferromagnetic body with both ends cone-shaped in the center of this figure will be levitated by the magnetic force. Five sensors are fixed to measure the desired state variables from this system. The magnetic force is applied to the ferromagnetic body in the perpendicular direction. It is separated into the X-axis direction and its perpendicular direction component, and is applied to the motion of the ferromagnetic body with five degrees of freedom.

The resolver has no relation to the control motion. When the controller operates it will measure the rotational motion about the X-axis. Table 1 lists the modeling parameter values of the system that will be used in the simulation and experiment. The slope angle of the cone-shaped body was designed to be 26.57[deg] so that control force can be applied to each mode equally. The self-inductance(L) of the electromagnet was obtained by using the parameter identification technique.
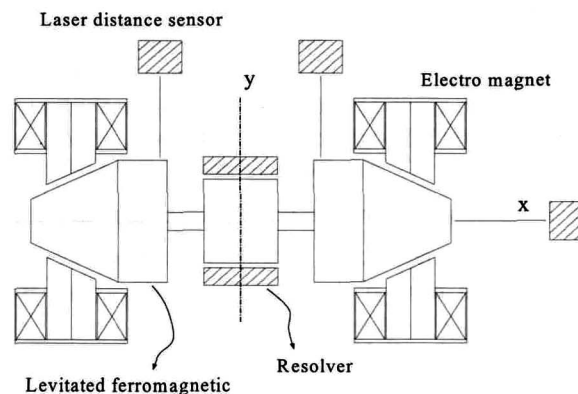

Fig. 1. System Configuration

Table 1. MODELING VALUE

	Description	value	unit
M	mass	0.696	kg
I	moment of inertia	2.4e-03	kg$\ast m^2$
α	slope angle of cone	26.57	deg.
ϕ	geometric parameter	77.55	deg.
a	geometric parameter	46.00e-03	m
h1	moment arm, X-dir	18.94e-03	m
h2	moment arm, Y-dir	67.89e-03	m
Amp	voltage gain of power amplifier	1	V/V
R	internal + current detect resistor	2.759+0.1	Ω
L	self-inductance of coil	0.043	H
d	gap at equilibrium point	1.0e-03	m
I_0	bias current	2.0	A

2.2 Equations of Motion

We assume the following to derive the equations of motion:
- The magnetic body is a rigid body and moves through an infinitesimal displacement around the equilibrium point.
- The self- inductance (L) of the electromagnet is constant and has no relation to the interval distance and the change of magnetic flux around the equilibrium point.
- Eight electromagnets have the same properties, also the power amplifiers to actuate the eight channels are the same.
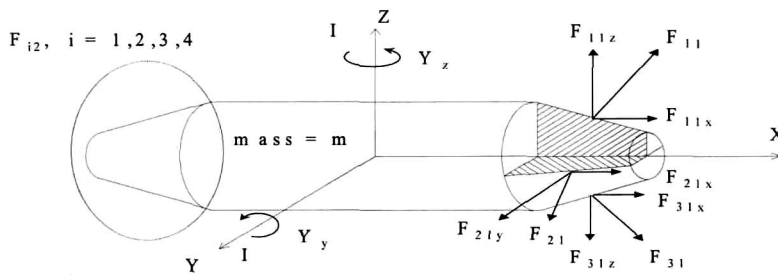

Fig. 2. Modeling of Magnetic Body

The magnetic force of each electromagnet has the following relations.

$$F_{ij} = kAN^P \frac{I_{ij}^n}{d_{ij}^m} = 0.27 \frac{I_{ij}^{1.97}}{d_{ij}^{1.10}}$$

I = Current [A],   d = Interval distance[mm],

Fij = Force [Kg_f]

(1)

Where k, A, N^P mean the turn, area, and permittivity, respectively.

The sucking force equation of the electromagnet can be obtained by measuring the load of the load cell current and distance repeatedly in the static state. So we can obtain equation (1) with a proper unit conversion. If no acceleration exists on the system, the magnetic force and the motion of the magnetic body including gravity can be expressed as equations (2) based on Fig.2.

$$m\ddot{x} = \sum_{k=1}^{4}(F_{k1x} - F_{k2x})$$

$$m\ddot{y} = \sum_{k=1}^{2}(F_{2ky} - F_{4ky})$$

$$m\ddot{z} = \sum_{k=1}^{2}(F_{1kz} - F_{3kz}) \tag{2}$$

$$\ddot{\theta}_x = 0$$

$$I\ddot{\theta}_y = h_2(F_{11z} + F_{32z} - F_{12z} - F_{31z}) + h_1(F_{12x} + F_{31x} - F_{11x} - F_{32x})$$

$$I\ddot{\theta}_z = h_2(F_{41y} + F_{22y} - F_{42y} - F_{21y}) + h_1(F_{21x} + F_{42x} - F_{41x} - F_{22x})$$

First, to design the control system, we must find the translation and rotation position in the center of the magnetic body from the fixed five displacement sensors. We can then find the interval distances between each of the electromagnets and the magnetic body by using the position values.

We can find the X, Z axis direction translation and Y axis direction rotation through the displacement sensors #1, #2, #4 in the X-Z plane of Fig. 3. The displacement sensors #1, #3, #5 are used in the X-Y plane. The motion of the magnetic body in the X-Y plane induces the error of the observation equation in the X-Z plane, but we assume the effect is very small because of the infinitesimal displacement. If we linearize these equations to obtain the control law, the nonlinear terms can be eliminated. The measured distance l_1, l_2, l_4 can be known, and we can find the
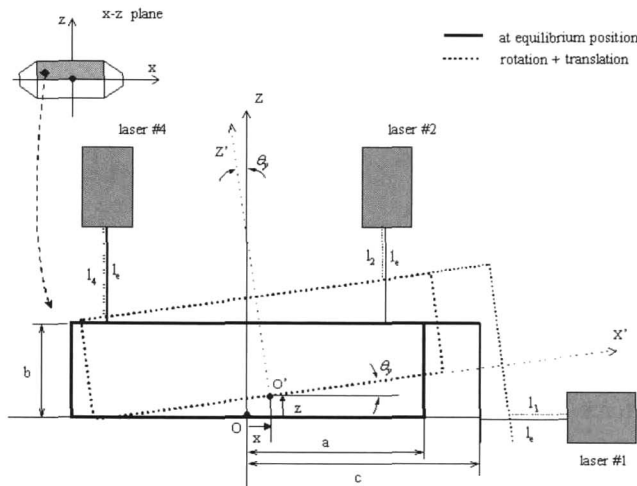

Fig. 3. Translation and Rotation Observation

infinitesimal x, z, θ_y about the translation and rotation from the measured value. From Fig. 3, equations (3) can be driven by the geometric consideration.

$$l_e + b = l_2 + (a - x)\tan\theta_y + \frac{b}{\cos\theta_y} + z$$

$$l_e + b = l_4 - (a + x)\tan\theta_y + \frac{b}{\cos\theta_y} + z \qquad (3)$$

$$l_e + c = l_1 + z\tan\theta_y + \frac{c}{\cos\theta_y} + x$$

Because of the infinitesimal displacement motion, these equations can be approximated as $\cos\theta_y \cong 1$, $\tan\theta_y \cong \theta_y$ and linearized based on the average distance of the sensors. We can then obtain equations (4).

$$x = l_e - l_1$$

$$z = l_e - \frac{1}{2}(l_2 + l_4)$$

$$\theta_y = \frac{l_4 - l_2}{2a} \qquad (4)$$

In the X-Y plane we can get the observation equation by the same method and then obtain a simple equation, such as equation (5), by redefining the distance information from the displacement sensors.

$$\begin{bmatrix} x \\ y \\ z \\ \theta_y \\ \theta_z \end{bmatrix} = \begin{bmatrix} 1 & 0 & 0 & 0 & 0 \\ 0 & 0 & \frac{1}{2} & 0 & \frac{1}{2} \\ 0 & \frac{1}{2} & 0 & \frac{1}{2} & 0 \\ 0 & \frac{1}{2a} & 0 & -\frac{1}{2a} & 0 \\ 0 & 0 & -\frac{1}{2a} & 0 & \frac{1}{2a} \end{bmatrix} \begin{bmatrix} \delta_1 \\ \delta_2 \\ \delta_3 \\ \delta_4 \\ \delta_5 \end{bmatrix} \qquad (5)$$

$$\delta_i = l_e - l_i \quad , \quad i = 1, 2, 3, 4, 5$$

Also, we need the relative equations between each electromagnet, which depends on the translation and rotation of the center of the magnetic body, and the distance of the surface of inclination. First, we assume the following:

· The surface where the electromagnet and the magnetic body face is constant.

· The line of action of the magnetic force is the same as the perpendicular line to the electromagnet surface at its point of bisection. Therefore, this line of action doesn't move on the fixed coordinates of the magnetic compensation system.

For the infinitesimal displacement of the magnetic body, we can think of each case of translational and rotational motion at the center of mass of the magnetic body. We derive the related equations for each motion and the whole related equations are obtained as equations (6) by superposition. Distance, d, is the distance from the equilibrium point. Each of the eight electromagnets has the same parameter values. Also d_{ij} is the distance between each of the electromagnets and varies by translational and rotational motion. l is defined as $\frac{m_1}{\theta_y}$ or $\frac{m_2}{\theta_z}$.

where, $\psi \cong 90 - \phi$ [deg] , $d_{ij} = f_{ij}(x, y, z, \theta_y, \theta_z)$, α means the inclination angle between the electromagnet and the magnetic body.

$$d_{11} = d - (\sin \alpha)x - (\cos \alpha)z - l \cos(\psi + \alpha)\theta_y$$
$$d_{21} = d - (\sin \alpha)x - (\cos \alpha)y + l \cos(\psi + \alpha)\theta_z$$
$$d_{31} = d - (\sin \alpha)x + (\cos \alpha)z + l \cos(\psi + \alpha)\theta_z$$
$$d_{41} = d - (\sin \alpha)x + (\cos \alpha)y - l \cos(\psi + \alpha)\theta_y$$
$$d_{12} = d + (\sin \alpha)x - (\cos \alpha)z + l \cos(\psi + \alpha)\theta_y \qquad (6)$$
$$d_{22} = d + (\sin \alpha)x - (\cos \alpha)y - l \cos(\psi + \alpha)\theta_z$$
$$d_{32} = d + (\sin \alpha)x + (\cos \alpha)z - l \cos(\psi + \alpha)\theta_y$$
$$d_{42} = d + (\sin \alpha)x + (\cos \alpha)y + l \cos(\psi + \alpha)\theta_z$$

Equations (7) show the relation of the distances and the current, respectively.

$$d_{ij} = d + r_{ij} \ , \ I_{ij} = I_0 + i_{ij} \qquad (7)$$

Here, d and I_0 are the average distance and the bias current, respectively. The nonlinear terms are caused by the magnetic force of the electromagnet, so that by linearizing equation (1) at this point the following linear equations are obtained:

$$F_{11} = c_1 i_{11} + c_2 x + c_3 z + c_4 \theta_y + 1.051$$
$$F_{21} = c_1 i_{21} + c_2 x + c_3 z - c_4 \theta_z + 1.051$$
$$F_{31} = c_1 i_{31} + c_2 x - c_3 z - c_4 \theta_y + 1.051$$
$$F_{41} = c_1 i_{41} + c_2 x - c_3 z + c_4 \theta_z + 1.051$$
$$F_{12} = c_1 i_{12} - c_2 x + c_3 z - c_4 \theta_y + 1.051 \qquad (8)$$
$$F_{22} = c_1 i_{22} - c_2 x + c_3 z + c_4 \theta_z + 1.051$$
$$F_{32} = c_1 i_{32} - c_2 x - c_3 z + c_4 \theta_y + 1.051$$
$$F_{42} = c_1 i_{42} - c_2 x - c_3 z - c_4 \theta_z + 1.051$$

where $c_1 \sim c_4$ are the linearization coefficients.

Finally, the following equation can be obtained from these results and equations (2).

$$M \ddot{\underline{\eta}} = \Gamma \underline{i} + P \underline{\eta}$$

where, $\underline{\eta} = \begin{bmatrix} x & y & z & \theta_y & \theta_z \end{bmatrix}^T$

$$\underline{i} = \begin{bmatrix} i_{11} & i_{21} & i_{31} & i_{41} & i_{12} & i_{22} & i_{32} & i_{42} \end{bmatrix}^T$$

M = Inertia Matrix $\qquad (9)$

Γ = Current Stiffness Matrix

P = Position Stiffness Matrix

2.3 State Equation and Mode Separation

The actuator for this system consists of the power amplifier and the electromagnet. The control output must be converted into voltage and the magnetic force is induced by current around the coil. The control voltage and the current around the coil have a delay effect due to the magnetic impedance of the electromagnet. When the voltage is applied, the current caused by the electromagnet is represented by the following equations (9).

$$\underline{v} = L \frac{d\underline{i}}{dt} + \underline{i}R \ , \qquad T(s) = \frac{1}{Ls + R}$$

From equation (9), there is a time delay between the control output voltage and the

magnetic force. Since equations (9) were not considered in designing the controller, the system will be unstable. In this research, by designing the analog power amplifier as a part of the actuator, using the current feedback and the lead compensator, we perform the voltage-current transfer delay compensation that is widely known. This system, as the inner loop, is includedin the whole magnetic levitation system. If we assume that the pole of the system is more influential than thepole of the actuator, the following state equations can be obtained by approximation.

$$\underline{i} \cong \frac{1}{R}\underline{v}$$
$$M\underline{\ddot{\eta}} = \frac{1}{R}\Gamma\underline{u}' + P\underline{\eta} + M\underline{a}$$

where, $\quad \underline{u}' = \begin{bmatrix} v_{11} & v_{21} & v_{31} & v_{41} & v_{12} & v_{22} & v_{32} & v_{42} \end{bmatrix}^T$ $\hspace{1cm}$ (10)

$$\underline{a} = \begin{bmatrix} a_x & a_y & a_z & \alpha_y & \alpha_z \end{bmatrix}^T$$

Equation (8) is rewritten as equations (10) for the voltage input($\underline{u}'$) and includes the gravity and the acceleration disturbance($\underline{a}$). From equations (10), the following equations can be obtained

$$\underline{\dot{x}}(t) = A\underline{x}(t) + B'\underline{u}'(t) + E\underline{f}(t)$$
$$\underline{y}(t) = C\underline{x}(t)$$

where, $\quad \underline{x} \in R^{10}, \quad \underline{u}' \in R^8, \quad \underline{f} \in R^5, \quad \underline{y} \in R^5$ $\hspace{1cm}$ (11)

$$\underline{x} = \begin{bmatrix} x_1, & x_2, & \cdots & x_{10} \end{bmatrix}^T = \begin{bmatrix} x, & \dot{x}, & y, & \dot{y}, & z, & \dot{z}, & \theta_y, & \dot{\theta}_y, & \theta_z, & \dot{\theta}_z \end{bmatrix}^T$$
$$\underline{y} = \begin{bmatrix} y_1, & \cdots & y_5 \end{bmatrix}^T = \begin{bmatrix} x, & y, & z, & \theta_y, & \theta_z \end{bmatrix}^T$$
$$\underline{u}' = \underline{v}, \quad \underline{f} = \underline{a}$$

The particular matrices can be expanded as;

$$A = \begin{bmatrix}
0 & 1 & 0 & 0 & 0 & 0 & 0 & 0 & 0 & 0 \\
\frac{8c_2 \sin \alpha}{m} & 0 & 0 & 0 & 0 & 0 & 0 & 0 & 0 & 0 \\
0 & 0 & 0 & 1 & 0 & 0 & 0 & 0 & 0 & 0 \\
0 & 0 & \frac{4c_3 \cos \alpha}{m} & 0 & 0 & 0 & 0 & 0 & 0 & 0 \\
0 & 0 & 0 & 0 & 0 & 1 & 0 & 0 & 0 & 0 \\
0 & 0 & 0 & 0 & \frac{4c_3 \cos \alpha}{m} & 0 & 0 & 0 & 0 & 0 \\
0 & 0 & 0 & 0 & 0 & 0 & 0 & 1 & 0 & 0 \\
0 & 0 & 0 & 0 & 0 & 0 & \frac{g_2}{I} & 0 & 0 & 0 \\
0 & 0 & 0 & 0 & 0 & 0 & 0 & 0 & 0 & 1 \\
0 & 0 & 0 & 0 & 0 & 0 & 0 & 0 & \frac{g_2}{I} & 0
\end{bmatrix}$$

$$E = \begin{bmatrix}
0 & 0 & 0 & 0 & 0 \\
1 & 0 & 0 & 0 & 0 \\
0 & 0 & 0 & 0 & 0 \\
0 & 1 & 0 & 0 & 0 \\
0 & 0 & 0 & 0 & 0 \\
0 & 0 & 1 & 0 & 0 \\
0 & 0 & 0 & 0 & 0 \\
0 & 0 & 0 & 1 & 0 \\
0 & 0 & 0 & 0 & 0 \\
0 & 0 & 0 & 0 & 1
\end{bmatrix}, \quad
C = \begin{bmatrix}
1 & 0 & 0 & 0 & 0 & 0 & 0 & 0 & 0 & 0 \\
0 & 0 & 1 & 0 & 0 & 0 & 0 & 0 & 0 & 0 \\
0 & 0 & 0 & 0 & 1 & 0 & 0 & 0 & 0 & 0 \\
0 & 0 & 0 & 0 & 0 & 0 & 1 & 0 & 0 & 0 \\
0 & 0 & 0 & 0 & 0 & 0 & 0 & 0 & 1 & 0
\end{bmatrix}$$

$$B' = \begin{bmatrix} 0 & 0 & 0 & 0 & 0 & 0 & 0 & 0 \\ \dfrac{c_1 \sin\alpha}{mR} & '' & '' & '' & '' & '' & '' & '' \\ 0 & 0 & 0 & 0 & 0 & 0 & 0 & 0 \\ 0 & \dfrac{c_1\cos\alpha}{mR} & 0 & \dfrac{-c_1\cos\alpha}{mR} & 0 & \dfrac{c_1\cos\alpha}{mR} & 0 & \dfrac{-c_1\cos\alpha}{mR} \\ 0 & 0 & 0 & 0 & 0 & 0 & 0 & 0 \\ \dfrac{c_1\cos\alpha}{mR} & 0 & \dfrac{-c_1\cos\alpha}{mR} & 0 & \dfrac{c_1\cos\alpha}{mR} & 0 & \dfrac{-c_1\cos\alpha}{mR} & 0 \\ 0 & 0 & 0 & 0 & 0 & 0 & 0 & 0 \\ \dfrac{g_1}{IR} & 0 & \dfrac{-g_1}{IR} & 0 & \dfrac{-g_1}{IR} & 0 & \dfrac{g_1}{IR} & 0 \\ 0 & 0 & 0 & 0 & 0 & 0 & 0 & 0 \\ 0 & \dfrac{-g_1}{IR} & 0 & \dfrac{g_1}{IR} & 0 & \dfrac{g_1}{IR} & 0 & \dfrac{-g_1}{IR} \end{bmatrix}$$

Equations (11) represent a controllable, observable and asymptotically unstable system. Also the system matrix is not coupled, but the input matrix couples the system. In this research, we think of the application of the acceleration sensor in the translational axis direction and want to design the controller to reject the disturbance. So if this system is separated, the controller design is relatively simple. Therefore we can find that the independent control inputs transferred in each mode are five from the fact that the raw direction rank of input matrix B′ are five. By replacing the control input matrix with equations (12), this system becomes uncoupled.

$$B\underline{u} = B'M_s\,\underline{u} = B'\begin{bmatrix} 1 & 0 & 1 & 1 & 0 \\ 1 & 1 & 0 & 0 & -1 \\ 1 & 0 & -1 & -1 & 0 \\ 1 & -1 & 0 & 0 & 1 \\ -1 & 0 & 1 & -1 & 0 \\ -1 & 1 & 0 & 0 & 1 \\ -1 & 0 & -1 & 1 & 0 \\ -1 & -1 & 0 & 0 & -1 \end{bmatrix}\underline{u} \tag{12}$$

$$\underline{u} = \begin{bmatrix} u_x, & u_y, & u_z, & u_{\theta_y}, & u_{\theta_z} \end{bmatrix}^T$$

where M_s is a matrix for mode separation.

By this method and the input vector $\underline{u}$, the state equation separates and the X-axis direction translational mode and the other mode can be obtained as equations (13) (Shin et al., 1994; Chen, 1995).

$$\frac{d}{dt}\begin{bmatrix} \underline{x}_a \\ \underline{x}_b \end{bmatrix} = \begin{bmatrix} A_a & 0 \\ 0 & A_b \end{bmatrix}\begin{bmatrix} \underline{x}_a \\ \underline{x}_b \end{bmatrix} +$$
$$\begin{bmatrix} b_a & 0 \\ 0 & B_b \end{bmatrix}\begin{bmatrix} u_a \\ \underline{u}_b \end{bmatrix} + \begin{bmatrix} e_a & 0 \\ 0 & E_b \end{bmatrix}\begin{bmatrix} f_a \\ \underline{f}_b \end{bmatrix} \tag{13}$$
$$\underline{y} = C\underline{x}, \quad \underline{x} = \begin{bmatrix} \underline{x}_a^T, \underline{x}_b^T \end{bmatrix}^T$$

The X-axis direction translational motion, and the remaining two-axis direction

translational and rotational motions can be separated as in equations(14) and equations(15).

$$\dot{\underline{x}}_a = A_a \underline{x}_a + b_a u_a + e_a f_a \tag{14}$$
$$y_a = x_1 = x$$

$$\dot{\underline{x}}_b = A_b \underline{x}_b + B_b \underline{u}_b + E_b \underline{f}_b$$
$$\underline{y}_b = C_b \underline{x} = \begin{bmatrix} y, & z, & \theta_y, & \theta_z \end{bmatrix}^T \tag{15}$$

Controller Design

3.1 The Complete System Block Diagram

The block diagram is shown in Fig. 4 to explain the whole system structure. The plant to be controlled is separated with the x-axis direction translational mode and the two other direction translational and rotational modes. In equations (14), the state feedback system is designed with a desired damping ratio, and natural frequency, and has the character of the acceleration sensor by using the current stiffness and the position stiffness. In equations (15) the controller concerned with the disturbance rejection ability, stability, robustness and low sensitivity of sensor must be designed. The effect of self-inductance (L) is neglected in equations (10), but actually in between the control output and plant input, the system includes the loop for the voltage-current delay compensator. As the model based compensator, we apply the LQG/LTR method (Kim, 1992; Lewis, 1963). This method enables us to estimate the state by the Kalman filter loop without information of the full state. But in the case of the X-axis direction translation mode, the state feedback is adapted and the state estimator is designed from the information of the X-axis direction position.
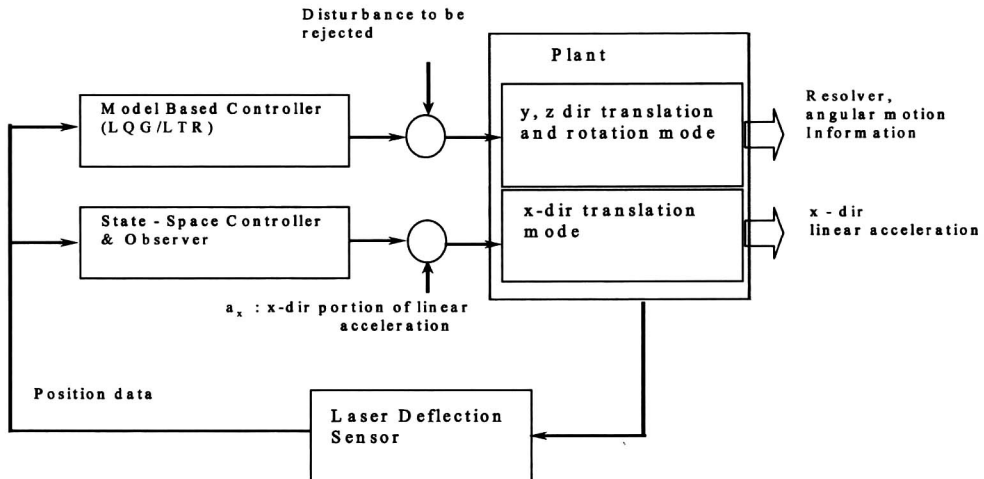
Fig. 4. The Complete System Block Diagram

3.2 Voltage-Current Delay Compensator

The objectives of the controller design are to reduced the time delay, and let input of the amplifier be maintained within appropriate limit. Lead compensator is performed. The gain margin

and the phase margin of the compensated system are infinitive, and the poles of system are located at −181.9 and −56.3, zero of system is positioned at −50. Without the compensation, 0.0104(sec) of time delay and 9.375(A/sec) in slew-rate occurredfor unit step input. However, through the simulation and the experiment, 0.0037(sec) time delay and 28(A/sec) slew-rate were obtained with compensation (Carr, 1991).

3.3 Acceleration Measurement System Design

For any second order system, the displacement of the system indicates the acceleration, if we design the system to produce a higher natural frequency than that of the signal to be measured. Since equations (14) represent a second order system, first we modelize simply the X-axis direction translational motion to obtain the second order system and then decide the desired natural frequency and damping ratio. The feedback gain can then be obtained in comparison with the characteristic equation by applying state feedback techniques in equations (15). Also the deadbeat observer is designed to make the full state feedback from the X-axis direction position information.

Fig. 5 shows simply the X-axis direction translation motion of the magnetic levitation system. Variables η_1, η_2 are used to derive the equation. As shown in the picture, the difference between η_1 and η_2 is the same as the first term, $x_1 = x$, the state vector of equations (13). The acceleration applied to the magnetic levitation system from outside is $\ddot{\eta}_1$. We assume that the relative motions of η_1 and η_2 include the damping(c) and stiffness (k). We obtain equation (16) in Fig. 5 (Thomson, 1972).

$$m\ddot{\eta}_2 = -c(\dot{\eta}_2 - \dot{\eta}_1) - k(\eta_2 - \eta_1) \tag{16}$$
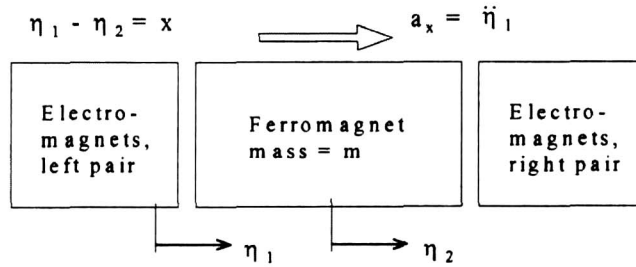
Fig. 5. X-axis Direction Translation Motion

If η_1 is a sinusoidal wave, position and acceleration are shown as equation(17).

$$\eta_1 = N \sin \omega t, \quad \ddot{\eta}_1 = -N\omega^2 \sin \omega t \tag{17}$$

Let $\eta_2 - \eta_1 = x$ in Fig.6, equations (18) can be obtained.

$$\ddot{x} + \frac{c}{m}\dot{x} + \frac{k}{m}x = N\omega^2 \sin \omega t \tag{18}$$

The solution of equation (18) is shown as

$$\frac{x}{N} = \frac{(\frac{\omega}{\omega_n})^2}{\sqrt{[1 - (\frac{\omega}{\omega_n})^2]^2 + (2\zeta \frac{\omega}{\omega_n})^2}} \tag{19}$$

$$\tan \Phi = \frac{2\xi(\frac{\omega}{\omega_n})^2}{1-(\frac{\omega}{\omega_n})^2}, \quad \zeta = \frac{c}{c_c}, \quad \omega_n = \sqrt{\frac{k}{m}}$$

Suppose that the system results in a higher natural frequency (ω_n) in comparison with the frequency of the signal to be measured (ω). Let $\omega/\omega_n \to 0$, then equations (19) is shown as

$$x \cong \frac{\omega^2 N}{\omega_n^2} = \frac{accelerati\ on}{\omega_n^2} \tag{20}$$

That is, within the range $\omega < \omega_n$, x is proportional to the acceleration with the rate of $(1/\omega_n^2)$. The natural frequency, ω_n, and damping ratio, ζ, are important design parameters.

The X-axis direction state, equations (14) performs state feedback with control law as equation (21). The controller then must be designed with the natural frequency and damping ratio that is desired in the system of Fig. 5.

$$u_a = K\underline{x}_a = \begin{bmatrix} \alpha_1 & \alpha_2 \end{bmatrix}\begin{bmatrix} x \\ \dot{x} \end{bmatrix} \tag{21}$$

The following second order differential equation can be obtained by using Table 1 in equation (14) and equation(21).

$$\ddot{x} - 18361\ \alpha_2\dot{x} - (26222 + 18361\ \alpha_1)x = f_a \tag{22}$$

In equation (22), by comparing equation (18) with equation (22), the coefficients α_1, α_2 should be determined so as to produce the natural frequency and the damping ratio desired in equation (18).

For the case of the acceleration sensor used in inertial measurement, the natural frequency of the system was designed to result in a comparatively low value. If the plant does not measure the sudden change of acceleration, the precise measurement is possible in measurable bandwidth. In this research, the natural frequency is designed to result in a low value, but there are design constraint conditions to be considered. That is, to approximate the magnetic levitated system as the second differential equation of equation (22), the pole of the power amplifier, included in the inner loop of the system, should be neglected. Therefore, the pole of the system in equations (14) and equation (22) must dominate over the minimum pole of the power amplifier. We should also be careful when the natural frequency and damping ratio is selected, because the pole gets close to the pole of the power amplifier if the natural frequency is made to be high in equation (18) (Lee, 1997).

In this study, the pole of equations (14) is designed to reach a value of $-16.336\pm j19.099$. Also, $\omega_n = 4[Hz]$, $\zeta = 0.65$. Examine Fig. 6. This figure shows the sensitivity plot versus frequency at the given natural frequency. In the case of $\zeta = 0.7$, we can obtain the acceleration with a small error of 0.01% with the indication value up to 0.2 times of natural frequency. If $\zeta < 0.7$, the measurement bandwidth becomes wider, but the error of indication value becomes larger. Hence, this system is designed to make the measurable bandwidth as wide as possible. The indication value has a $\pm1.22\%$ error and the measurable bandwidth is $0\sim2.45[Hz]$. The phase of frequency ratio, ω/ω_n, must be 0 or proportionally increased to reconstruct the signal without shape distortion. In case of $\zeta = 0$, the phase is zero, at $\zeta = 0.7$, the phase increases regularly in the range of $0<\omega/\omega_n<1$. In Fig. 7, where $\zeta = 0.65$, there is minimal distortion but the measurable bandwidth becomes wide. In Fig. 6, the measurement sensitivity is the following.

· Sensitivity : $1.58314 \times 10^{-3} [mm \ / \ mm \ / \ \sec^2]$ with ±1.22%, max. at frequency range 0~2.45[Hz]

Therefore, for the case of a step disturbance input with the acceleration of $500 [mm \ / \ \sec^2]$ to the X-axis direction is applied, the displacement of 0.79157[mm] happens in steady state.

To apply the control input as equation (21), we need the full state of the system. The displacement, X, can be obtained from the sensor. This $\dot{x}$ can be obtained by differentiating. However, if the signal including the measurement noise is differentiated, the differentiated values we desire can't be obtained because the noise of the high frequency area is amplified. Generally, the solution of this method is to design the observer. Because if the observer includes the dynamics of the system, the high frequency signal is decreased. We also considered the digital controller for the system. First, we discretize equations(14).

We assume there is no acceleration disturbance. The discrete state space equation from Equations (14) is shown as follows

$$\underline{x}_{a,k+1} = A_a^s \underline{x}_{a,k} + \underline{b}_a^s u_a$$
$$y_{a,k} = \underline{c}_a \underline{x}_{a,k}$$

(23)
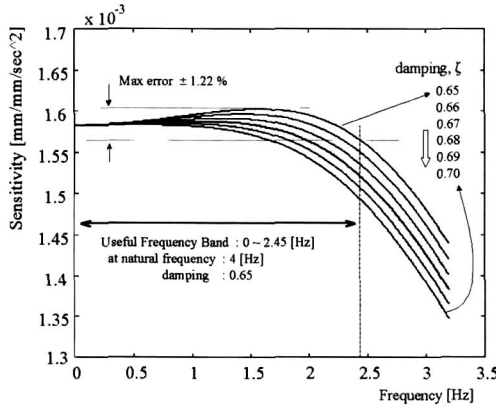
Fig. 6. Sensitivity Plot
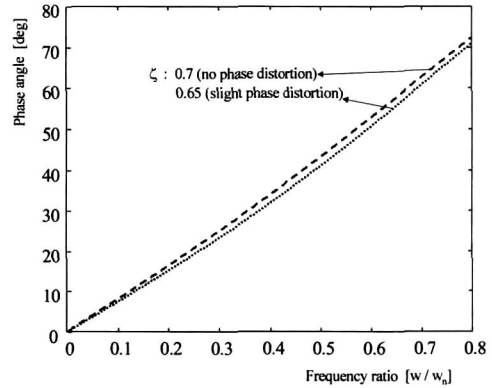
Fig. 7. Phase Angle Plot

Let the state vector estimated by the state estimator $\hat{\underline{x}}_{a,k}$. Dynamics of the state estimator based on control input, output and state equation is shown as equation (22)) (Lee, 1997).

$$\hat{\underline{x}}_{a,k+1} = (A_a^s - L\underline{c}_a) \hat{\underline{x}}_{a,k} + \underline{b}_a^s u_k + L y_{a,k}$$

(24)

The estimator gain is $L = [L_1 \quad L_2]^T$, L_1, L_2 are scalar balers. The estimator error is defined as $\tilde{y}_{a,k} = y_{a,k} - \hat{y}_{a,k}$. $A_{a,0} = A_a^s - L\underline{c}_a$ is the estimator state matrix. The estimator characteristic polynomial is shown as equation (25).

$$\Delta_0(z) = \left| zI - A_{a,0} \right|$$

(25)

Because this system is observable, L can be determined such that the estimator state matrix, $A_{a,0}$, have the pole at z=0. Then, the estimator error becomes zero after the n sample period. Characteristics of the observer are defined with $\Delta^D(z) = z^n = z^2$. Comparing

coefficients with equation (25), the estimator is designed as follows:

$$L_1 = 2.026222 \quad , \quad L_2 = 1.048642 \ e^3$$

This method is for the deadbeat observer design.

$$\begin{bmatrix} \hat{x}_{1k+1} \\ \hat{x}_{2k+1} \end{bmatrix} = \begin{bmatrix} 1.0131112 & 0.0010044 \\ 26.3369994 & 1.0131112 \end{bmatrix} \begin{bmatrix} \hat{x}_{1k} \\ \hat{x}_{2k} \end{bmatrix} +$$

$$\begin{bmatrix} 0.0091803 \\ 18.4419004 \end{bmatrix} \begin{bmatrix} u_k \end{bmatrix} + \begin{bmatrix} L_1 \\ L_2 \end{bmatrix} (y_{k+1} - \hat{x}_k)$$

The initial condition is $\hat{x}_{1k}(0) = \hat{x}_{2k}(0) = 0$.

Fig. 8 is the block diagram for simulation when the X-axis direction acceleration exists. Fig. 9 shows the tested time response. The result could be obtained as expected and we also know the control input was applied properly(Kim, 2000; Cho et al., 2002).
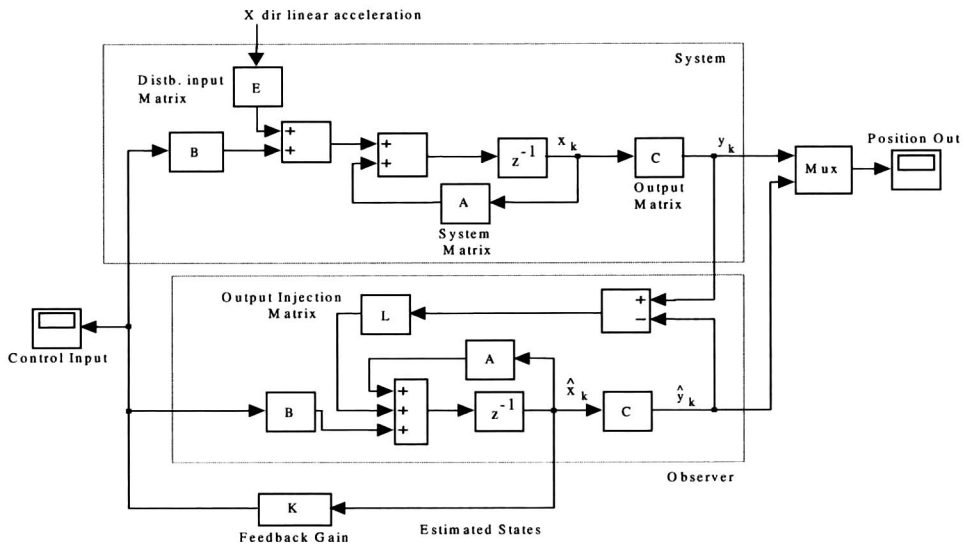
Fig. 8. Acceleration Measurement System
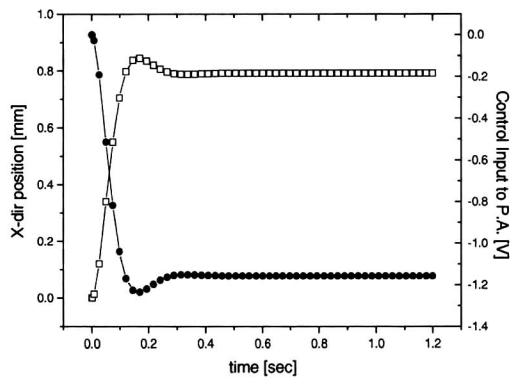
Fig. 9. Time Response

3.4 Disturbance Rejection Controller Design

The state equations, which describe the Y, Z-axis direction translational and rotational motion, are equations (15). The requirements of the controller are:
  - Steady state error is zero, if the disturbance is constant
  - Disturbance rejection at bandwidth 0~16[Hz]
  - Low sensitivity character of sensor noise at bandwidth is more than 160[Hz]
  - Stability, robustness of the model error

Since this system is nonsingular and minimum phase, by using LQG/LTR, the acceleration disturbance is eliminated and the low sensitivity of the sensor noise, as well as stability and robustness are considered. The designed plant model that includes the free integral factor is shown as equations (26). This equation does not consider the steady state error with the constant disturbance.

$$\dot{x} = Ax + Bu$$
$$y = Cx$$

$$x = \begin{bmatrix} u_b^T & x_b^T \end{bmatrix}^T , \quad u = \dot{u}_b$$

$$A = \begin{bmatrix} 0 & 0 \\ B_b & A_b \end{bmatrix} , \quad B = \begin{bmatrix} I \\ 0 \end{bmatrix} , \quad C = \begin{bmatrix} 0 & C_b \end{bmatrix} \tag{26}$$

The transfer function matrix of the LQG/LTR compensator is shown as

$$K(s) = G(sI - A + BG + HC)^{-1}H \tag{27}$$

The parameter, H, can be obtained through the designing of the target filter loop. Also, G, through the designing of the loop transfer recovery.

With the LQG/LTR control system design, including plant noise and sensor noise(assumed as white noise), the state equations for the design plant are shown as follows:

$$\dot{x} = Ax + Bu + L\xi$$
$$y = Cx + \theta$$

$$E[\xi(t)] = E[\theta(t)] = 0$$
$$E[\xi(t)\xi(\tau)^T] = I\delta(t - \tau) \tag{28}$$
$$E[\theta(t)\theta(\tau)^T] = \mu I\delta(t - \tau)$$

Here ξ and θ are zero mean white noise vectors with strengths $I, \mu I$. μ and L are design parameters. Since the free integral is included, L can be used with equation (27) so that the singular values in the range of low frequency and high frequency coincide.

$$L = \begin{bmatrix} -\left[C_b A_b^{-1} B_b\right]^{-1} \\ C^T\left[C_b C_b^T\right]^{-1} \end{bmatrix} \tag{29}$$

Fig. 10 is the target filter loop, which is satisfied with the given conditions. From this figure, the target filter loop is designed to have the disturbance rejection ability in the frequency range of 0~16[Hz] and to have the low sensitivity ability of the sensor noise in the range of more than 160[Hz]. Generally, the acceleration disturbance, which should be eliminated in the system, has the energy from the low frequency range. The effect of sensor noise is distributed widely in the very high frequency range. The singular value, depending on the frequency in the target filter loop, satisfies the requested capability.
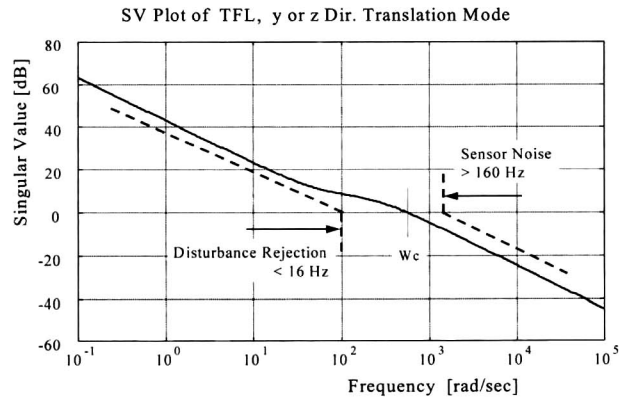
SV Plot of TFL, y or z Dir. Translation Mode

Fig. 10. Target Filter Loop

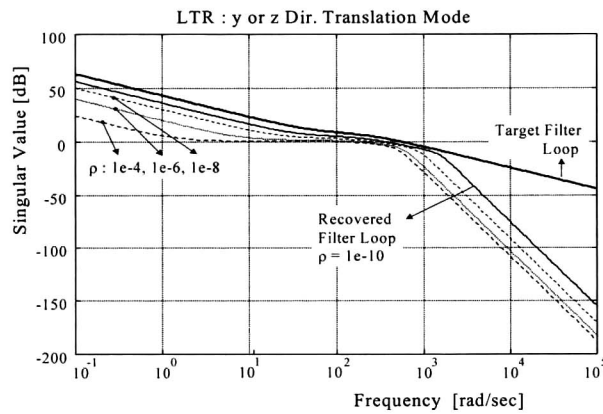LTR : y or z Dir. Translation Mode

Fig. 11. Loop Transfer Recovery
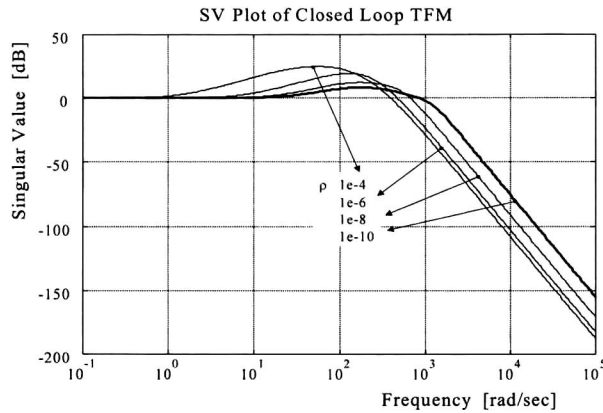
SV Plot of Closed Loop TFM

Fig. 12. Closed Loop Singular Value Plot

Through the loop transfer recovery, the compensated system is recovered to the target filter loop. The loop transfer recovery is possible by solving the LQR control problem. Because of the

minimum phase plant, if the loop transfer recovery parameter ρ approximates to zero, a good recovery can be expected. Actually, considering a possible control force on the system, the value selected to be recovered corresponds to 6~9 times the cross over frequency. When the value of ρ is the order of 10^{-10}, a good loop transfer recovery is performed as in Fig. 11. Fig. 12 is the compensated closed loop singular value plot and provides the criterion to decide stability and robustness.

Simulations are performed in the time domain. To determine the capability of the designed system the following conditions are used.

· Sensor noise: The covariance based on the measurement data from the laser displacement sensor was obtained and mean is $\sigma^2 = 0.1642 \; X10^{-7}$ at zero mean.

· Process noise, acceleration disturbance: Process disturbance was not considered in the simulation. Acceleration disturbance was estimated about a step input with random strength. Disturbance strength is not constant. If constant, the response of the system was investigated.

In Fig. 13, when the disturbance is applied constantly, the disturbance rejection ability can be seen. The disturbance will be applied approximately up to $25[m/\sec^2]$. Fig. 14shows that in the case when the sampling period is sufficiently small, the control input can be applied to the power amplifier of the actual plant. We know that the control input is possible within the proper range and also the high level disturbance is well controlled.

In the case where the input is a ramp (increasing constantly), the steady state output is kept constant in a state where there is a small departure from the equilibrium point. In the case where this system is used to measure the angular motion of a body, the body's acceleration increases constantly. In the worst case, if the second or higher order function is kept constant for sometime, it will be outof the equilibrium point or be an unstable state. That is not a problem, because the acceleration to be rejected represented a vibrational state or the rate of change of acceleration is not significantly large.
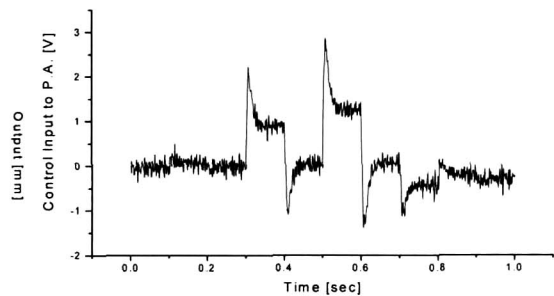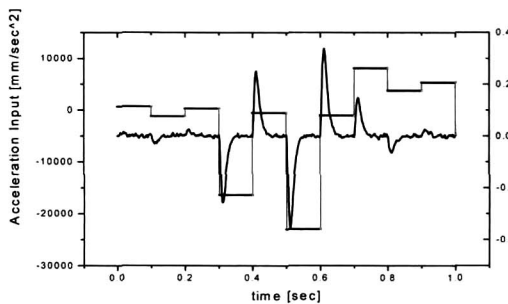

Fig. 13. Time Response for Disturbance Input   Fig. 14. Control Input Applied to PowerAmplifier

Results and Discussion

By using the frictionless supporting character of the magnetic levitation, we suggested a new method of measuring linear acceleration and rotational motion of an airplane or space vehicle etc. By using the specific parameter modeling values in table 1, we did the system modeling and designed the controller using state feedback and the model-based compensator techniques. We assumed the power amplifier from the lead compensator and current feedback circuit compensates the delay effect of the self-inductance.

There are three ways for undertaking the controller design problem. First, the power amplifier and the electromagnet controller design using the current feedback and the lead compensator were performed for the voltage-current transfer delay compensation. Without the

compensation, 0.0104(sec) of time delay and 9.375(A/sec) in slew-rate occurred. However, through the simulation and the experiment, 0.0037(sec) time delay and 28(A/sec) slew-rate were obtained with compensation. Second, the acceleration measurement system of the X-axis translation mode was designed. In this controller design, the system performed within 0 ~ 2.45(Hz) of the measurable bandwidth, 1.58314×10^{-3}(mm/mm/sec$^{2)}$) in sensitivity, and ±1.22% maximum indication error within the bandwidth. Third, the controllers for the Y-axis and Z-axis direction translational and rotational modes were designed for disturbance rejection and stability/robustness. As the model based compensator, the LQG/LTR method was applied. The designed system showed that disturbance was rejected within 0 ~ 16(Hz) frequency range. Also it has a low sensitivity character for sensor noise above 160(Hz).

The modeling parameter values of this system are obtained by experiment. Therefore, there is room to improve by optimizing the modeling parameter values and doing further research on preventing an energy loss by using a hybrid method, super-conduct coil, etc.

References

1. J.S.Choi, Y.S.Baek, "A Single DOF Magnetic Levitation System using Time Delay Control and Reduced-Order Observer", *KSME International Journal*, 2002, pp.1643-1651.

2. K.H.Park, K.B.Choi, S.H.Kim, Y.K.Kwak, "Design of Magnetically Suspended Frictionless Manipulator", *KSME International Journal*, 1995, pp.323-335

3. Park, Y.O., Han, J.Y. and Bang, H.C.",An Application of Levitation Systems into a 3-axis Attitude Detector", *proceeding of the 13th Korean Automatic Control Conference*, 1998, pp.1891-1894

4. Jung, H.S., "Six Degree of Freedom precision Motion Control of the Frictionless Positioning Device Suspended by Cone-Shaped Active Magnetic Bearings", Human tech Thesis Prize, The 2nd Award Papers, 1998, pp.65-75.

5. Shin, Y.J., Cho, Y.C., Oh, M.S. and Cho, K.R., "Initial Alignment of INS under Random Disturbance", *Journal of The Korean Society for Aeronautics and Space in Korea,* November. 1994, pp.177-183.

6. Chen, Chi-Tsong*, Linear System Theory and Design*, Oxford University Press Inc., 1995.

7. Kim, J.S., *Linear Control System Engineering*, Cheong Moon Gak Publishing, 1992.

8. Lewis, Frank L., *Applied Optimal Control and Estimation*, Prentice Hall, 1963.

9. Carr, Joseph J., *"Designers Handbook of Instrumentation and Control Circuits"*, Academic Press, Inc., 1991.

10. Thomson, William T., *Theory of Vibration with Application*, Prentice Hall, 1972.

11. Lee, Jun-Ho, "Experimental Evaluation of Q-parameterization Controllers to a Magnetic Bearing with Imbalance", *T.IEE Japan*, Vol.177-D, No.10, 1997.

12. Kim, Y.D., "Development of Inertial Measurement Sensor Using Magnetic Levitation", M.S. Thesis, Pusan National University, Korea, 2000.

13. Cho, K.R., Bainum, P.M., Kim, Y.D., and Tan, Zhaozhi, "Development of Inertial Measurement Sensor Using Magnetic Levitation",AAS Paper 02-106, January 2002.